Crosstalk in oxygen homeostasis networks: SKN-1/NRF inhibits the HIF-1 hypoxia-inducible factor in *Caenorhabditis elegans*

Dingxia Feng*¶, Zhiwei Zhai¶, Zhiyong Shao, Yi Zhang, and Jo Anne Powell-Coffman*

Department of Genetics, Development and Cell Biology, Iowa State University, Ames, Iowa, United States of America

*corresponding author:

E-mail: japc@iastate.edu (JP)

E-mail: fengdi@indiana.edu (DF)

¶co-first authors contributed equally

Abstract

During development, homeostasis, and disease, organisms must balance responses that allow adaptation to low oxygen (hypoxia) with those that protect cells from oxidative stress. The evolutionarily conserved hypoxia-inducible factors are central to these processes, as they orchestrate transcriptional responses to oxygen deprivation. Here, we employ genetic strategies in *C. elegans* to identify stress-responsive genes and pathways that modulate the HIF-1 hypoxia-inducible factor and facilitate oxygen homeostasis. Through a genome-wide RNAi screen, we show that RNAi-mediated mitochondrial or proteasomal dysfunction increases the expression of hypoxia-responsive reporter *Pnhr-57:GFP* in *C. elegans*. Interestingly, only a subset of these effects requires *hif-1*. Of particular importance, we found that *skn-1* RNAi increases the expression of hypoxia-responsive reporter *Pnhr-57:GFP* and elevates HIF-1 protein levels. The SKN-1/NRF transcription factor has been shown to promote oxidative stress resistance. We present evidence that the crosstalk between HIF-1 and SKN-1 is mediated by EGL-9, the prolyl hydroxylase that targets HIF-1 for oxygen-dependent degradation. Treatment that induces SKN-1, such as heat, increases expression of a *Pegl-9:GFP* reporter, and this effect requires *skn-1* function and a putative SKN-1 binding site in *egl-9* regulatory sequences. Collectively, these data support a model in which SKN-1 promotes *egl-9* transcription, thereby inhibiting HIF-1. We propose that this interaction enables animals to adapt quickly to changes in cellular oxygenation and to better survive accompanying oxidative stress.

Introduction

Oxygen homeostasis has profound effects on health and fitness. Oxygen serves as the terminal electron acceptor in the oxidative phosphorylation processes that generate energy for life. When

42 oxygen levels are low (hypoxia), cells and tissues must adapt quickly by increasing oxygen
43 delivery, adjusting the levels of key metabolic enzymes, and limiting the accumulation of
44 misfolded proteins. While oxygen is essential, it is also highly reactive. The reactive oxygen
45 species (ROS) generated by cellular metabolism and signaling processes can damage
46 macromolecules, and excess ROS are thought to contribute to cellular aging and deterioration [1-
47 3]. One of the central challenges of aerobic life is to coordinate the biological networks that
48 control disparate aspects of oxygen homeostasis.
49 This balance between surviving hypoxic stress and mitigating the potential damage caused by
50 reactive oxygen species is especially important in cardiovascular development and disease.
51 When ischemia blocks circulation to a mammalian tissue, oxygen levels drop, and cells induce
52 hypoxia-inducible transcription factors (HIFs). Upon reperfusion and reoxygenation of the tissue,
53 mammalian cells respond by rapidly degrading HIF and inducing the NRF2 transcription factor
54 [4, 5]. However, intermittent hypoxia has been shown to induce both HIF-1α and NRF2 [6, 7].
55 NRF2 activates phase II detoxification genes to mitigate the effects of oxidative insults [8, 9].
56 Although mammalian HIF and NRF2 share some common target genes such as aldehyde
57 dehydrogenase 1A1 or heme oxygenase-1 HO-1, the genes induced by re-oxygenation are
58 largely distinct from those that respond to oxygen deprivation [5, 10, 11]. Crosstalk between
59 these two pathways is complex and context specific in mammals [12], as these important
60 transcription factors facilitate the rapid changes in gene expression needed to limit reperfusion
61 injury and regulate oxygen-dependent developmental processes.
62 *C. elegans* has been proven to be an excellent model system for studying the regulatory networks
63 that govern oxygen homeostasis. The *C. elegans* genome encodes a single hypoxia-inducible
64 factor alpha subunit (HIF-1), and the *hif-1* gene has been shown to have important roles in stress

65 response and in aging [13-17]. HIF protein levels and HIF activity are tightly regulated. When
66 oxygen is abundant, the HIF alpha subunit is hydroxylated by the PHD/EGL-9 enzymes. Once
67 modified, HIFα protein interacts with the Von Hippel-Lindau tumor suppressor (VHL) and is
68 targeted for ubiquitination and proteasomal degradation [18-23]. Thus, in hypoxic conditions,
69 HIF-1 protein is stable, and the transcription factor complex can activate the expression of a
70 battery of genes that enable adaptation to low oxygen. This pathway for oxygen-dependent
71 degradation of HIF protein is evolutionarily conserved. The *C. elegans hif-1, aha-1, egl-9,* and
72 *vhl-1* genes are orthologous to mammalian *HIFα*, *HIFβ*, *PHD*, and *VHL*, respectively [24-26].
73 The targets of *C. elegans* HIF-1 include *egl-9* and *rhy-1*, genes that inhibit HIF-1 expression and
74 activity [27-30]. In wild-type animals, these negative feedback loops keep HIF-1 activity in
75 check and limit the potentially adverse effects of HIF-1 over-activation.
76 The *C. elegans skn-1* gene is homologous to mammalian *NRF1/2/3* [31]. SKN-1 regulates the
77 expression of a battery of genes with cytoprotective functions, including phase II detoxification
78 genes [32, 33]. SKN-1 is activated by a range of stresses or toxicants that cause oxidative stress,
79 and SKN-1 promotes resistance to these insults [32, 34-37].
80 Here, we investigate the cellular processes and transcriptional networks that regulate HIF-1
81 function. We describe an unbiased genetic screen to identify genes that inhibit *C. elegans* HIF-1.
82 We discover that SKN-1/NRF represses HIF-1 protein levels. Hence, SKN-1-mediated repression
83 of HIF-1 may provide a mechanism by which cells can rapidly respond to specific environmental
84 stresses and optimize gene expression to achieve oxygen homeostasis. We investigate the
85 hypothesis that this cross talk is mediated by EGL-9, the oxygen-sensing prolyl hydroxylase that
86 modulates HIF-1 stability and activity.

Results

To identify genes and cellular processes that attenuated HIF-1-mediated gene expression, we conducted a genome-wide RNAi screen. This experimental strategy relied on the *Pnhr-57:GFP* reporter gene, which had been shown to be responsive to HIF-1 and hypoxia [28, 29]. Through chromatin immunoprecipitation experiments, we confirmed that *nhr-57* was a direct target of HIF-1 (S1 Fig). We screened a bacterial RNAi library representing ~80% of *C. elegans* genes [38], and we identified 179 genes for which RNAi increased *Pnhr-57:GFP* expression, as assayed by inspection under a fluorescent stereomicroscope (screen design illustrated in Fig 1A). These genes are listed in S1 Table and their functions are summarized in Fig 1B. Remarkably, 89 genes were predicted to have mitochondrial or metabolic functions, and the majority of these were electron transport chain components (42 genes) or subunits of mitochondrial ribosomes (24 genes). The second largest category of the genes was protein folding or turnover (33 genes), and the majority of these were proteasomal components. The remaining major categories include vesicular transport, transporters and channels, signaling and cytoskeleton, transcription and DNA or RNA processing.

Fig 1. Genome-wide RNAi screen to identify negative regulators of HIF-1-mediated gene expression. (A) Illustration of screen design. The screen identified RNAi treatments that increased the expression of *Pnhr-57:GFP*, a reporter that has been shown to be induced by hypoxia and positively regulated by HIF-1. (B) Functional summary of the 179 genes identified from the RNAi screen.

Recognizing that most eukaryotic genes are coordinately regulated by multiple transcription

110 factors, we did a secondary screen to identify those RNAi treatments that had a clear *hif-1*-
111 dependent effect on *Pnhr-57:GFP* expression. To do this, we compared the *Pnhr-57:GFP*
112 induction of these 179 RNAi treatments in wild-type animals and *hif-1*-deficient animals. Most
113 of the 179 RNAi treatments increased the expression of *Pnhr-57:GFP* independent of *hif-1*.
114 However, the *Pnhr-57:GFP* induction by 13 RNAi treatments showed a strong *hif-1*-dependent
115 effect (S2 Table). Among these 13 genes, as expected, RNAi for *egl-9, rhy-1*, and *vhl-1*,
116 previously characterized negative regulators of *C. elegans* HIF-1 [26, 29], increased *Pnhr-*
117 *57:GFP* expression in wild-type animals, but not in *hif-1* mutants. These results validated the
118 efficacy of our screen approach, and gave us the confidence to continue investigating the
119 potentially new negative regulators of HIF-1 among these 13 genes.

120 *skn-1* attenuates HIF-1 protein levels and HIF-1 function

121 We were especially intrigued by the finding that *skn-1* RNAi increased the expression of HIF-1-
122 responsive reporter. Transcription factor SKN-1 has been shown to have critical roles in enabling
123 *C. elegans* to respond to oxidative stress [32-34, 39]. Our finding suggested a potential crosstalk
124 between hypoxia response and oxidative stress response. To quantify the effect of *skn-1* RNAi
125 on this HIF-1-responsive reporter, we examined *Pnhr-57:*GFP levels using protein blots. In the
126 normal room air culture conditions, *Pnhr-57:*GFP was 40% higher in *skn-1* RNAi compared to
127 control RNAi (Fig 2A) (**$p < 0.01$, from three independent experiments). To gain insight to the
128 effects of this interaction in hypoxic conditions, we moved the animals to 0.5% oxygen. After 4
129 hours of hypoxia treatment, *Pnhr-57:*GFP was 50% higher in *skn-1* RNAi compared to control
130 RNAi (Fig 2A) (**$p < 0.01$, from three independent experiments). Thus, *skn-1* RNAi increased
131 *Pnhr-57:*GFP levels under normoxic and hypoxic conditions.
132 We next asked whether *skn-1* RNAi increased HIF-1 protein levels. We tested two *skn-1* RNAi

133 constructs, and each resulted in an increase of HIF-1 protein levels by 2 to 3-fold as shown in Fig
134 2B (**$p < 0.01$, from three independent experiments). In sum, these results showed that *skn-1*
135 RNAi increased HIF-1 protein level and HIF-1 reporter expression.
136
137 **Fig 2. Identification of SKN-1 as a regulator of HIF-1.** (A) *skn-1* RNAi increased expression
138 of the *Pnhr-57:GFP* reporter. Reporter gene expression was quantitated in L4-stage animals in
139 normal culture conditions or after 2 or 4 hours of hypoxia treatment (0.5% oxygen). The protein
140 levels were calculated from three independent experiments and normalized to 0 hour hypoxia
141 control RNAi. A representative western blot is shown. In each lane, lysates from 80 L4-satge
142 worms were loaded. Asterisks indicate significant differences between control RNAi and *skn-*
143 *1* RNAi at any given time point. *: $p < 0.05$; **: $p < 0.01$. (B) *skn-1* RNAi increased HIF-1
144 protein levels. These animals expressed an epitope-tagged HIF-1 protein [40]. The protein levels
145 were calculated from three independent experiments and normalized to control RNAi. Two
146 different RNAi clones were assayed, and they are designated as *skn-1(1)* and *skn-1(2)* here. A
147 representative western blot is shown. In each lane, lysates from 100 L4-satge worms were
148 loaded. Asterisks indicate significant differences between control RNAi and *skn-1* RNAi at any
149 given time point. **: $p < 0.01$.
150

151 Differential requirements for *skn-1* and *hif-1*

152 The finding that SKN-1 repressed HIF-1 protein levels suggested that there might be conditions
153 in which it would be beneficial for the animal to express one of these two stress-responsive
154 transcription factors, but not the other. To address this, we examined the relative requirements
155 for *skn-1* and *hif-1* more closely.

156 In previous studies, we and others had shown that *hif-1* was required for survival in moderate
157 hypoxia [25, 41]. As validated in the experiments described in Table 1, loss of *hif-1* impaired
158 animal development and survival in 0.5% oxygen: after 24 hours of hypoxia treatment, only
159 75.8% of *hif-1*-deficient eggs hatched, and only 25.6% developed to adulthood within 72 hours.
160 In contrast, *skn-1* RNAi had no effect on *C. elegans* development and survival in hypoxic
161 conditions: after 24 hours of hypoxia treatment, 99.4% of *skn-1* RNAi treated eggs hatched and
162 completed normal development to adulthood within 72 hours.
163

164 **Table 1. Relative requirements for *skn-1* and *hif-1*: survival in 0.5% oxygen.**
165

Genotype	**% hatched ± SEM**	**% survive to adult ± SEM**	**n [a]**
N2 (wild type)	99.1 ± 0.25	99.1± 0.3	672
hif-1(ia04)	75.8 ± 2.5	25.6 ± 0.9	616
N2;control(RNAi)	99.6 ± 0.19	99.6 ± 0.2	558
N2;*skn-1(RNAi)*	99.4 ± 0.42	99.4 ± 0.4	640

166 [a] n is the total number of animals assayed in three independent experiments.
167

168 Prior studies also suggested that there were differential requirements for HIF-1 and SKN-1 in
169 oxidative stress conditions. Mutants carrying loss-of-function mutations in *skn-1* have been
170 shown to decrease the ability of *C. elegans* to survive exposure to agents that cause oxidative
171 stress [34, 42-44]. In contrast, *C. elegans* carrying loss-of-function mutations in *hif-1* have been
172 reported to be relatively resistant to peroxide [40]. We compared these phenotypes directly, and
173 the data are provided in Table 2. These experiments confirmed that, while *skn-1*-deficient
174 animals were sensitive to t-butyl peroxide, mutants lacking *hif-1* were remarkably resistant to
175 this oxidative stress: while none of the *skn-1*-deficient mutants survived 6 hours of t-butyl

176 peroxide treatment, 97.5% of *hif-1*-deficient mutants survived 10 hours of t-butyl peroxide

177 treatment.

178

179 **Table 2. Relative requirements for *skn-1* and *hif-1*: survival on t-butyl-peroxide.**

180

Exposure time	Genotype	Mean Survival ± SEM	N [a]
6 hours	N2 (wild type)	95.2 ± 2.6	106
	skn-1(zu67)	0.0 ± 0	117
	hif-1(ia04)	100.0 ± 0	120
8 hours	N2 (wild type)	29.08 ± 7.7	106
	skn-1(zu67)	0.0 ± 0	117
	hif-1(ia04)	99.17 ± 0.8	120
10 hours	N2 (wild type)	2.78 ± 2.8	106
	skn-1(zu67)	0.0 ± 0	117
	hif-1(ia04)	97.50 ± 2.5	120

181 [a] n is the total number of animals assayed in three independent experiments.

182

183 # SKN-1/NRF promotes *egl-9* expression

184 We next sought to discover the mechanism by which SKN-1 inhibits HIF-1 protein levels. In

185 silico analyses identified a potential SKN-1 binding site in the *egl-9* promoter region (Fig 3A).

186 EGL-9 is a central inhibitor of HIF-1 protein levels [26, 27] and of HIF-1 transcriptional activity

187 [29, 30]. This suggested a model in which the SKN-1 DNA-binding complex bound directly to

188 the *egl-9* regulatory sequences to promote *egl-9* expression, which, in turn, would ultimately

189 decrease HIF-1 protein levels. To test this, we employed real-time quantitative RT-PCR to

190 compare *egl-9* mRNA levels in worms fed with *skn-1* RNAi versus control RNAi. To produce

191 reliable and reproducible results, *egl-9* mRNA levels were quantitated in three independent real-
192 time quantitative RT-PCR experiments in L4-stage animals in room air or hypoxic conditions
193 (0.5% oxygen). Each sample was performed with three technical replicates, and they produced
194 similar C_t values. There are seven isoforms of *egl-9* mRNA transcripts
195 (https://wormbase.org/species/c_elegans/gene/WBGene00001178#0-9f-10). The real-time
196 quantitative PCR primer set used in this study can detect six *egl-9* mRNA isoforms. In room air,
197 *skn-1* RNAi decreased *egl-9* mRNA levels by 30% compared to control RNAi (**$p < 0.01$, from
198 three independent experiments) (Fig 3B). HIF-1 has been shown to activate *egl-9* mRNA
199 expression under hypoxia, creating a negative feedback loop [27, 28]. In accordance with this,
200 the inhibition effects of *skn-1* RNAi on *egl-9* mRNA levels were minimized by placing the
201 animals in hypoxic conditions (Fig 3B).
202
203 **Fig 3. Identification of *egl-9* as a potential transcriptional target of SKN-1.** (A) Sequence
204 from the *egl-9* promoter was aligned with established SKN-1 binding sites in *gcs-1*, *med-1*,
205 and *med-2*. Asterisks identify sequence identities shared by all four promoter regions in this
206 interval, and predicted SKN-1 binding sites are in red. (B) *skn-1* RNAi decreased *egl-9* mRNA
207 levels. *egl-9* mRNA levels were quantitated from three independent real-time quantitative RT-
208 PCR experiments. The values at each time point were normalized to the 0 hour hypoxia control
209 RNAi. Asterisks indicate significant differences between control RNAi and *skn-1* RNAi at any
210 given time point. *: $p < 0.05$; **: $p < 0.01$.
211
212 To test the hypothesis that conditions that activate SKN-1 can promote *egl-9* promoter activity,
213 we generated a reporter construct in which 1.6 kb of *egl-9* regulatory sequence directed the

214 expression of GFP (Fig 4A). To distinguish the effects of SKN-1 on *egl-9* expression from those
215 of HIF-1, we conducted these experiments in a *hif-1* mutant background. In agreement with prior
216 studies [45], *Pegl-9:*GFP was visible in several tissues, including the body muscle, vulva,
217 pharynx, anterior intestine, rectal cells and additional cells in the tail in standard culture
218 conditions (20 °C) (Figs 4B and 4C). When the animals were treated with heat shock conditions
219 that had been shown to activate SKN-1 (29 °C for 20 hours) [34], we observed dramatic
220 induction of *Pegl-9:*GFP in the intestine. (Figs 4D and 4E).
221
222 **Fig 4. Heat shock alters *Pegl-9:GFP* expression.** (A) The *Pegl-9:GFP* construct includes 1.6
223 kb of sequence 5' to the *egl-9* translational start. GFP coding sequence is diagramed as a green
224 box. The red oval indicates the position of the putative SKN-1 binding site. (B-E) *Pegl-*
225 *9:GFP* expression in L4-stage animals under normal culture conditions and heat shock. Animals
226 are shown as DIC images (B and D) and corresponding images of GFP fluorescence (C and E).
227 In all images, the head is to the right. (B and C) Under normal conditions, *Pegl-9:GFP* was
228 expressed in the body muscle, vulva, pharynx, anterior intestine, rectal cells and additional cells
229 in the tail. (D and E) After heat shock treatment (29°C for 20 hours), *Pegl-9:GFP* was strongly
230 induced in the intestine. The*Pegl-9:GFP* expression patterns in the L1, L2, L3 and adults were
231 similar to that in the L4 worms, under both normal and heat shock conditions (data not shown).
232
233 We next asked whether heat shock induction of *Pegl-9:GFP* required *skn-1* function. We found
234 that heat shock increased *Pegl-9:*GFP by 2.5-fold in animals carrying the wild-type *skn-1* allele.
235 However, the heat shock induction of *Pegl-9:GFP* was abolished in *skn-1(zu67)* loss-of-function
236 mutants (Fig 5A). Analyses of another independent *Pegl-9:GFP* transgenic line yielded similar

237 results (data not shown).

238 To test the hypothesis that the putative SKN-1 binding site in the *egl-9* promoter was required for
239 heat shock induction of *Pegl-9:GFP*, we generated the *P(m)egl-9:GFP* construct, which
240 contained mutations in the putative SKN-1 binding site (in red type in Fig 3A). Heat shock
241 increased *Pegl-9:*GFP by 2.1-fold. However, heat shock failed to induce the expression of
242 *P(m)egl-9:GFP* (Fig 5B). Experiments with a second *P(m)egl-9:GFP* transgenic line gave
243 similar results (data not shown). Collectively, these data demonstrated that heat shock induction
244 of *Pegl-9:GFP* required *skn-1* function and the putative SKN-1 binding site in the *egl-9*
245 promoter.

246

247 **Fig 5. SKN-1 acts through the putative SKN-1 binding site in the *egl-9* promoter to**
248 **activate *egl-9* expression.** (A) Heat shock induced *Pegl-9:GFP* in animals carrying the wild-
249 type s*kn-1* allele, but did not induce the reporter in animals carrying the *skn-1(zu67)* loss-of-
250 function mutation. The vertical axis shows the log2 fold changes of GFP caused by heat shock
251 for each strain with standard errors, as determined by four biological replicates. A representative
252 western blot is shown. For each sample, 20 L4-satge worms were boiled and lysates
253 corresponding to 10 worms were loaded to each lane. (B) Heat shock increased the expression
254 of *Pegl-9*:*GFP*, but did not increase the expression of the reporter in which the putative SKN-1
255 binding site was mutated (*P(m)egl-9:GFP*). The vertical axis shows the log2 fold changes of
256 GFP caused by heat shock for each strain with standard errors, as determined by five biological
257 replicates. A representative western blot is shown. For each sample, 20 L4-satge worms were
258 boiled and lysates corresponding to 10 worms were loaded to each lane.

259

260 # Discussion

261 This study provides new insights to the mechanisms that allow animals to respond appropriately
262 to diverse stresses. While HIF-1 and SKN-1 are both stress responsive transcription factors, they
263 have distinct functions. For example, *skn-1*-deficient animals are less able to survive exposure to
264 peroxide, while *hif-1-deficient* mutants are relatively resistant to this oxidizing agent [40].
265 Conversely, while a deletion mutation in *hif-1* dramatically impairs survival in 0.5% oxygen
266 [25], *skn-1* RNAi has little effect (Table 1). Thus, animals may benefit from cross-talk between
267 these two transcription factors as they are challenged by oxygen deprivation and oxidative stress.
268 Here, we provide evidence that SKN-1 promotes *egl-9* expression, thereby attenuating HIF-1
269 function.

270 ## SKN-1 promotes *egl-9* expression, thereby inhibiting HIF-1

271 Our data support a model in which SKN-1 binds directly to the *egl-9* promoter to increase *egl-9*
272 expression. This conclusion is further substantiated by the genome wide chromatin
273 immunoprecipitation experiments that determined that SKN-1:GFP associated with DNA
274 sequences in the *egl-9* 5' regulatory region [46]. EGL-9 functions as a cellular oxygen sensor,
275 and it mediates oxygen-dependent degradation of HIF-1 [26]. Hence, *skn-1* RNAi results in
276 increased HIF-1 protein levels (Fig 2B). We expect that this regulatory interaction, in which
277 SKN-1 can quickly down-regulate HIF-1, would allow animals to adapt quickly to changes in
278 cellular conditions.
279 Prior studies have identified genes that are positively regulated by either SKN-1 or HIF-1, and
280 these gene lists are largely non-overlapping [28, 32, 47-49]. Genes that are commonly regulated
281 by both SKN-1 and HIF-1 include K10H10.2/*cysl-2*, F57B9.1, M05D6.5, and *rhy-1*. Two lines
282 of evidence suggest that *rhy-1* may be a direct target of SKN-1. First, Oliveira et al. (2009)

283 identified a potential SKN-1 binding site in the *rhy-1* promoter region. Second, the
284 modENCODE project found that *rhy-1* 5' regulatory sequences associated with SKN-1 *in vivo*
285 [46]. Like *egl-9, rhy-1* is also a negative regulator of HIF-1 [28, 29]. Collectively, these data
286 suggest that SKN-1 may act through both *egl-9* and *rhy-1* to reduce HIF-1 function.
287 Interactions between HIF-1 and SKN-1 are likely to be different in select cells, developmental
288 stages, or environmental contexts. HIF-1, EGL-9 and SKN-1 each have other developmental
289 functions, and some of these are specific to certain cell types [34, 50-54]. The downstream
290 effects of SKN-1 or HIF-1 activation are further influenced by cellular or environmental
291 contexts. For example, *C. elegans* SKN-1 can be activated by arsenite or by t-butyl
292 hydroperoxide, but only a subset of SKN-1 targets are activated by either toxicant [32]. Also,
293 while *C. elegans* SKN-1 and HIF-1 have distinct roles in peroxide and hypoxia stress responses,
294 their functions overlap in selenium and hydrogen sulfide stress responses [13, 15, 35-37].
295 Similarly, the mammalian NRF and HIF transcription factors are very sensitive to environmental
296 and physiological cues or stresses, and their regulatory relationships are context specific.
297 Ischemia causes tissue hypoxia, which stabilizes HIF transcription factors. Once the ischemic
298 tissue is reperfused, HIF transcription factors are degraded quickly and NRF2 is up-regulated,
299 presumably to limit the oxidative damage [4, 5]. However, intermittent hypoxia has been shown
300 to induce both HIF-1α and NRF2 [6, 7]. While NRF2 signaling activates HIF-1 in several cancer
301 types [12], studies of the anti-inflammatory drug andrographolide in endothelial cells revealed
302 interactions between NRF2 and the PHDs that modulate HIF-1 [55]. NRF2 and the HIF
303 transcription factors have key roles in angiogenesis and iron regulation, and their functions can
304 converge on developmental processes or feedback loops that modulate their activities [12, 56-
305 58].

306 ## *Pnhr-57:GFP* as a marker for hypoxia-induced gene expression:
307 ## discoveries and insights from a genome-wide screen

308 Prior studies have demonstrated that *nhr-57* was induced by hypoxia in a *hif-1*-dependent
309 manner and that over-expression of *Pnhr-57*:*GFP* in *egl-9* mutants required *hif-1* [13, 27-30].
310 Moreover, Bellier *et al*. (2009) found that HIF-1-mediated induction of *nhr-57* helped to protect
311 *C. elegans* from the lethal effects of pore-forming toxins [59]. While these studies showed that
312 *nhr-57* is a direct target of HIF-1, other transcription factors must also contribute to its
313 expression. The studies presented here show that, while genes such as *egl-9* or *rhy-1* clearly
314 regulate HIF-1 to control *Pnhr-57*:*GFP* expression, many other RNAi treatments can activate
315 *Pnhr-57*:*GFP* through *hif-1*-independent pathways. The *Pnhr-57*:*GFP* reporter will continue to
316 be a valuable marker, but these data inform our interpretations of studies that employ this
317 reporter. While *Pnhr-57*:*GFP* is clearly regulated by HIF-1, it is important to compare
318 expression of the reporter in wild-type and *hif-1*-deficient animals before drawing conclusions
319 about HIF-1 activity.
320 We found that diverse RNAi treatments that compromise metabolic function or protein
321 homeostasis increased *Pnhr-57*:*GFP* expression, and this effect did not require a functional *hif-1*
322 gene. Interestingly, many of the genes integral to these processes have been shown to have roles
323 in stress response and aging [60-65]. RNAi-mediated depletion of proteasomal components has
324 also been shown to impact resistance to polyglutamine toxicity and to induce expression of
325 *Pgpdh-1*:*GFP*, a marker for osmotic stress and glycerol production [66, 67].
326 Further characterization of the 179 RNAi treatments that increased *Pnhr-57*:GFP identified 13
327 genes that had much stronger effects in animals carrying a wild-type *hif-1* gene. These genes
328 included *vhl-1, egl-9,* and *rhy-1*. These three genes had all been identified in prior studies as

329 negative regulators of HIF-1 [26, 29]. The succinate dehydrogenase subunit *sdhb-1* was also
330 found to have *hif-1*-dependent effects. This is especially interesting, since studies in cancer cell
331 lines have shown that succinate can inhibit the enzymatic activities of HIF prolyl hydroxylases
332 [68, 69]. *sams-1* and *sbp-1* encode the *C. elegans* S-adenosyl methionine synthetase and the
333 SREBP homologs, respectively. The RNAi treatments of sams-1 and sbp-1 have a lesser impact
334 on *Pnhr-57*:GFP levels in *hif-1* mutants, suggesting that the effects of *sams-1* and *sbp-1* RNAi on
335 the reporter are mediated by HIF-1 (S2 Fig). Both of these genes have key roles in methionine
336 metabolism and fatty acid biosynthesis [70], and it will be interesting to investigate the ways in
337 which these important processes intersect with hypoxia response.

338 Materials and methods

339 Strains

340 The following strains were used in this study: wild-type N2 Bristol; ZG430: *Pnhr-*
341 *57:GFP(iaIs07)*IV; *egl-9(sa307)*V; *hif-1(ia04)*V; *Phif-1:hif-1a:Myc:HA (iaIs28)*; ZG120: *Pnhr-*
342 *57:GFP(iaIs07)*IV; ZG509: *rrf-3(pk1426)*II*; Pnhr-57:GFP(iaIs07)*IV; ZG508: *rrf-3(pk1426)*II;
343 *Pnhr-57:GFP(iaIs07)*IV; *hif-1(ia04)*V; ZG429: *hif-1(ia04)*V; *Phif-1:hif-1a:Myc:HA(iaIs28)*;
344 ZG472: *hif-1(ia04)*V; *Pegl-9:GFP(iaEx84);* ZG487: *hif-1(ia04)*V; *P(m)egl-9:GFP(iaEx96);*
345 ZG488: *skn-1(zu67)*IV; *hif-1(ia04)*V; *Pegl-9:GFP(iaEx84).* The transgenes expressing epitope-
346 tagged HIF-1 protein were described and characterized previously [40].

347 RNAi experiments

348 The RNAi screen was conducted as previously described [71], with few modifications. Each
349 bacterial clone (expressing double-stranded RNA for one gene) was cultured in L-broth with 50
350 ug/mL ampicillin and 12.5 ug/mL tetracycline overnight at 37°C. The following morning, the

351 bacteria were inoculated into new L-broth with 100 ug/mL ampicillin for 6 hours at 37°C before
352 seeding on 24-well NGM agar plates with 25 ug/mL carbenicillin and 2 mM IPTG. Each RNAi
353 clone was plated in duplicate. The following day, 15-25 L1-stage worms were added to each
354 well. The plates were incubated at 15°C for 5-6 days, and then the worms were screened for
355 positive *Pnhr-57:*GFP green fluorescence by stereomicroscopy. Bacterial RNAi clones that
356 increased the reporter were rescreened in two independent replicates, and the plasmid inserts
357 were validated by sequencing.
358 *skn-1* RNAi causes maternal-effect lethality, in this study we examined the effects of first
359 generation *skn-1* RNAi. Dead egg percentages given by the first generation *skn-1* RNAi adults
360 were measured to check the *skn-1* RNAi efficiency. We routinely achieved as high as 90% dead
361 egg percentages from the first generation *skn-1* RNAi adults, indicating high *skn-1* RNAi
362 efficiency.

363 Hypoxia stress and oxidative stress assays

364 To assess the relative effects of t-butyl-peroxide exposure, animals in the first day of adulthood
365 were placed on NGM plates containing 7.5 mM t-butyl-peroxide, in the presence of bacterial
366 food. The survival was scored after treating the animals for 6, 8 or 10 hours.
367 For hypoxia experiments, adults were allowed to lay eggs on standard NGM plates with OP50
368 bacterial food for 2 hours. The adults were then removed, and the plates with embryos were
369 placed in a hypoxia chamber (0.5% oxygen; 21°C) for 24 hours. After 24 hours, the plates were
370 removed from the hypoxia chamber, and the un-hatched eggs were counted immediately. The
371 plates were then maintained in room air (21°C). The adult worms were counted at 72 hour since
372 the eggs had been laid. Wild-type control animals hatched within 24 hours and reached
373 adulthood within 72 hours.

374 ## *Pegl-9:GFP* expression constructs

375 To generate the *Pegl-9:GFP* construct, a fragment that contained 1.6 kb of sequence upstream of
376 the initiation ATG of *egl-9* gene was amplified by PCR using the forward primer 5'-
377 CGCGCATGCGTGTATGTGTGTGAAAGAG-3' and the reverse primer 5'-
378 GCGGTCGACGCAACTTTTTTCTGTCACATTCAG-3'. The PCR product was cloned into the
379 green fluorescence protein (GFP) vector pPD95.75 (gift from Andrew Fire). To create the
380 *P(m)egl-9:GFP* point mutation construct, the predicted SKN-1 binding site TTTGTCAT [34,
381 72]was altered to CGACGGGC. Transgenic animals were generated by injection of DNA into
382 the gonadal syncitium, using standard methods with *rol-6* (pRF4) as the co-injection marker
383 [73]. For each construct, two independent transgenic lines were generated and assayed.

384 ## Protein Blots

385 To assay the expression of GFP or HIF-1 proteins, 20-100 L4-stage worms were collected and
386 boiled for 5 min in 1X SDS sample buffer, and the lysates were size fractionated on
387 polyacrylamide gels and analyzed by Western blots. The GFP-specific mouse monoclonal
388 antibody (from Roche) was used at 1:500. The HA-specific mouse monoclonal antibody (from
389 Cell Signaling) was used at 1:250. The secondary antibody (goat anti-mouse IgG+IgM from
390 Biorad) was used at 1:2000 dilutions. The western blot images were analyzed by the Image J
391 software. For each assay, three to five independent biological replicates were included.

392 ## RNA extraction and real-time quantitative RT-PCR

393 Total RNA was isolated from synchronized L4-stage animals using Trizol (Invitrogen) and
394 RNeasy Mini Kit (Qiagen). After being treated by RNase free DNase (Promega), total RNA was
395 reverse transcribed to complementary DNA using Oligo dT_{18} primer and AffinityScript reverse

396 transcriptase (Stratagene). Real-time quantitative PCR was performed using the iQ SYBR
397 GREEN supermix (Bio-Rad) and Stratagene Mx4000 multiplex PCR system. In the assay, three
398 biological replicates were included. And for each sample, three technical replicates were
399 performed and they gave similar C_t values. And cDNA from 62.5 ng of total RNA was added to
400 each PCR reaction. Relative mRNA quantification was performed using the efficiency-corrected
401 comparative quantification method [74]. *inf-1*, a gene not regulated by hypoxia, was used as the
402 reference gene [28]. The primer sequences for *inf-1* real-time quantitative PCR are included in
403 S1 Fig. The primers for *egl-9* real-time quantitative PCR are the forward primer 5'-
404 GCCGACTTTCAATCCACTTC-3' and reverse primer 5'- AATGATCGGAGATCGACTGG-
405 3'. There are seven isoforms of *egl-9* mRNA transcripts
406 (https://wormbase.org/species/c_elegans/gene/WBGene00001178#0-9f-10). This primer set can
407 detect six out of seven *egl-9* mRNA isoforms. The isoform d.1 will not be detected by this
408 primer set, because the forward primer is located within the eighth intron of the unspliced
409 isoform d.1.

410 **References**

411 1. Beckman KB, Ames BN. The free radical theory of aging matures. Physiol Rev. 1998;78(2):547-
412 81. Epub 1998/04/30. PubMed PMID: 9562038.
413 2. Finkel T. Oxidant signals and oxidative stress. Current opinion in cell biology. 2003;15(2):247-
414 54. Epub 2003/03/22. PubMed PMID: 12648682.
415 3. Finkel T, Holbrook NJ. Oxidants, oxidative stress and the biology of ageing. Nature.
416 2000;408(6809):239-47. Epub 2000/11/23. doi: 10.1038/35041687. PubMed PMID: 11089981.
417 4. Kim YJ, Ahn JY, Liang P, Ip C, Zhang Y, Park YM. Human prx1 gene is a target of Nrf2 and is
418 up-regulated by hypoxia/reoxygenation: implication to tumor biology. Cancer Res. 2007;67(2):546-54.
419 Epub 2007/01/20. doi: 67/2/546 [pii]
420 10.1158/0008-5472.CAN-06-2401. PubMed PMID: 17234762.
421 5. Leonard MO, Kieran NE, Howell K, Burne MJ, Varadarajan R, Dhakshinamoorthy S, et al.
422 Reoxygenation-specific activation of the antioxidant transcription factor Nrf2 mediates cytoprotective
423 gene expression in ischemia-reperfusion injury. FASEB journal : official publication of the Federation of
424 American Societies for Experimental Biology. 2006;20(14):2624-6. Epub 2006/12/05. doi: 10.1096/fj.06-
425 5097fje. PubMed PMID: 17142801.
426 6. Malec V, Gottschald OR, Li S, Rose F, Seeger W, Hanze J. HIF-1 alpha signaling is augmented
427 during intermittent hypoxia by induction of the Nrf2 pathway in NOX1-expressing adenocarcinoma A549

428 cells. Free radical biology & medicine. 2010;48(12):1626-35. Epub 2010/03/30. doi:
429 10.1016/j.freeradbiomed.2010.03.008. PubMed PMID: 20347035.
430 7. Martinive P, Defresne F, Bouzin C, Saliez J, Lair F, Gregoire V, et al. Preconditioning of the
431 tumor vasculature and tumor cells by intermittent hypoxia: implications for anticancer therapies. Cancer
432 Res. 2006;66(24):11736-44. doi: 10.1158/0008-5472.CAN-06-2056. PubMed PMID: 17178869.
433 8. Thimmulappa RK, Mai KH, Srisuma S, Kensler TW, Yamamoto M, Biswal S. Identification of
434 Nrf2-regulated genes induced by the chemopreventive agent sulforaphane by oligonucleotide microarray.
435 Cancer Res. 2002;62(18):5196-203. Epub 2002/09/18. PubMed PMID: 12234984.
436 9. Hayes JD, McMahon M. Molecular basis for the contribution of the antioxidant responsive
437 element to cancer chemoprevention. Cancer Lett. 2001;174(2):103-13. Epub 2001/11/02. doi:
438 S0304383501006954 [pii]. PubMed PMID: 11689285.
439 10. Hough RB, Piatigorsky J. Preferential transcription of rabbit Aldh1a1 in the cornea: implication
440 of hypoxia-related pathways. Molecular and cellular biology. 2004;24(3):1324-40. Epub 2004/01/20.
441 PubMed PMID: 14729976; PubMed Central PMCID: PMC321433.
442 11. Yeligar SM, Machida K, Kalra VK. Ethanol-induced HO-1 and NQO1 are differentially regulated
443 by HIF-1alpha and Nrf2 to attenuate inflammatory cytokine expression. The Journal of biological
444 chemistry. 2010;285(46):35359-73. Epub 2010/09/14. doi: 10.1074/jbc.M110.138636. PubMed PMID:
445 20833713; PubMed Central PMCID: PMC2975160.
446 12. Toth RK, Warfel NA. Strange Bedfellows: Nuclear Factor, Erythroid 2-Like 2 (Nrf2) and
447 Hypoxia-Inducible Factor 1 (HIF-1) in Tumor Hypoxia. Antioxidants (Basel). 2017;6(2). doi:
448 10.3390/antiox6020027. PubMed PMID: 28383481; PubMed Central PMCID: PMCPMC5488007.
449 13. Budde MW, Roth MB. Hydrogen sulfide increases hypoxia-inducible factor-1 activity
450 independently of von Hippel-Lindau tumor suppressor-1 in C. elegans. Mol Biol Cell. 2010;21(1):212-7.
451 Epub 2009/11/06. doi: E09-03-0199 [pii]
452 10.1091/mbc.E09-03-0199. PubMed PMID: 19889840; PubMed Central PMCID: PMC2801715.
453 14. Powell-Coffman JA. Hypoxia signaling and resistance in C. elegans. Trends Endocrinol Metab.
454 2010;21(7):435-40. Epub 2010/03/26. doi: S1043-2760(10)00041-X [pii]
455 10.1016/j.tem.2010.02.006. PubMed PMID: 20335046.
456 15. Romanelli-Credrez L, Doitsidou M, Alkema MJ, Salinas G. HIF-1 Has a Central Role in
457 Caenorhabditis elegans Organismal Response to Selenium. Front Genet. 2020;11:63. doi:
458 10.3389/fgene.2020.00063. PubMed PMID: 32161616; PubMed Central PMCID: PMCPMC7052493.
459 16. Saldanha JN, Parashar A, Pandey S, Powell-Coffman JA. Multiparameter behavioral analyses
460 provide insights to mechanisms of cyanide resistance in Caenorhabditis elegans. Toxicol Sci.
461 2013;135(1):156-68. doi: 10.1093/toxsci/kft138. PubMed PMID: 23805000; PubMed Central PMCID:
462 PMCPMC3748764.
463 17. Shao Z, Zhang Y, Ye Q, Saldanha JN, Powell-Coffman JA. C. elegans SWAN-1 Binds to EGL-9
464 and regulates HIF-1-mediated resistance to the bacterial pathogen Pseudomonas aeruginosa PAO1. PLoS
465 Pathog. 2010;6(8):e1001075. doi: 10.1371/journal.ppat.1001075. PubMed PMID: 20865124; PubMed
466 Central PMCID: PMCPMC2928816.
467 18. Kaelin WG, Jr., Ratcliffe PJ. Oxygen sensing by metazoans: the central role of the HIF
468 hydroxylase pathway. Mol Cell. 2008;30(4):393-402. Epub 2008/05/24. doi: S1097-2765(08)00292-X
469 [pii]
470 10.1016/j.molcel.2008.04.009. PubMed PMID: 18498744.
471 19. Semenza GL. Oxygen sensing, homeostasis, and disease. N Engl J Med. 2011;365(6):537-47. doi:
472 10.1056/NEJMra1011165. PubMed PMID: 21830968.
473 20. Wang GL, Jiang BH, Rue EA, Semenza GL. Hypoxia-inducible factor 1 is a basic-helix-loop-
474 helix-PAS heterodimer regulated by cellular O2 tension. Proc Natl Acad Sci U S A. 1995;92(12):5510-4.
475 doi: 10.1073/pnas.92.12.5510. PubMed PMID: 7539918; PubMed Central PMCID: PMCPMC41725.
476 21. Maxwell PH, Wiesener MS, Chang GW, Clifford SC, Vaux EC, Cockman ME, et al. The tumour
477 suppressor protein VHL targets hypoxia-inducible factors for oxygen-dependent proteolysis. Nature.
478 1999;399(6733):271-5. doi: 10.1038/20459. PubMed PMID: 10353251.

479 22. Jaakkola P, Mole DR, Tian YM, Wilson MI, Gielbert J, Gaskell SJ, et al. Targeting of HIF-alpha
480 to the von Hippel-Lindau ubiquitylation complex by O2-regulated prolyl hydroxylation. Science.
481 2001;292(5516):468-72. doi: 10.1126/science.1059796. PubMed PMID: 11292861.
482 23. Ivan M, Kondo K, Yang H, Kim W, Valiando J, Ohh M, et al. HIFalpha targeted for VHL-
483 mediated destruction by proline hydroxylation: implications for O2 sensing. Science.
484 2001;292(5516):464-8. doi: 10.1126/science.1059817. PubMed PMID: 11292862.
485 24. Powell-Coffman JA, Bradfield CA, Wood WB. Caenorhabditis elegans orthologs of the aryl
486 hydrocarbon receptor and its heterodimerization partner the aryl hydrocarbon receptor nuclear
487 translocator. Proc Natl Acad Sci U S A. 1998;95(6):2844-9. Epub 1998/04/18. PubMed PMID: 9501178.
488 25. Jiang H, Guo R, Powell-Coffman JA. The Caenorhabditis elegans hif-1 gene encodes a bHLH-
489 PAS protein that is required for adaptation to hypoxia. Proc Natl Acad Sci U S A. 2001;98(14):7916-21.
490 Epub 2001/06/28. doi: 10.1073/pnas.141234698
491 141234698 [pii]. PubMed PMID: 11427734; PubMed Central PMCID: PMC35443.
492 26. Epstein AC, Gleadle JM, McNeill LA, Hewitson KS, O'Rourke J, Mole DR, et al. C. elegans
493 EGL-9 and mammalian homologs define a family of dioxygenases that regulate HIF by prolyl
494 hydroxylation. Cell. 2001;107(1):43-54. Epub 2001/10/12. doi: S0092-8674(01)00507-4 [pii]. PubMed
495 PMID: 11595184.
496 27. Bishop T, Lau KW, Epstein AC, Kim SK, Jiang M, O'Rourke D, et al. Genetic analysis of
497 pathways regulated by the von Hippel-Lindau tumor suppressor in Caenorhabditis elegans. PLoS Biol.
498 2004;2(10):e289. Epub 2004/09/14. doi: 10.1371/journal.pbio.0020289. PubMed PMID: 15361934.
499 28. Shen C, Nettleton D, Jiang M, Kim SK, Powell-Coffman JA. Roles of the HIF-1 hypoxia-
500 inducible factor during hypoxia response in Caenorhabditis elegans. The Journal of biological chemistry.
501 2005;280(21):20580-8. Epub 2005/03/23. doi: M501894200 [pii]
502 10.1074/jbc.M501894200. PubMed PMID: 15781453.
503 29. Shen C, Shao Z, Powell-Coffman JA. The Caenorhabditis elegans rhy-1 gene inhibits HIF-1
504 hypoxia-inducible factor activity in a negative feedback loop that does not include vhl-1. Genetics.
505 2006;174(3):1205-14. Epub 2006/09/19. doi: genetics.106.063594 [pii]
506 10.1534/genetics.106.063594. PubMed PMID: 16980385.
507 30. Shao Z, Zhang Y, Powell-Coffman JA. Two distinct roles for EGL-9 in the regulation of HIF-1-
508 mediated gene expression in Caenorhabditis elegans. Genetics. 2009;183(3):821-9. Epub 2009/09/10. doi:
509 genetics.109.107284 [pii]
510 10.1534/genetics.109.107284. PubMed PMID: 19737748; PubMed Central PMCID: PMC2778979.
511 31. Walker AK, See R, Batchelder C, Kophengnavong T, Gronniger JT, Shi Y, et al. A conserved
512 transcription motif suggesting functional parallels between Caenorhabditis elegans SKN-1 and
513 Cap'n'Collar-related basic leucine zipper proteins. The Journal of biological chemistry.
514 2000;275(29):22166-71. Epub 2000/04/15. doi: 10.1074/jbc.M001746200
515 M001746200 [pii]. PubMed PMID: 10764775.
516 32. Oliveira RP, Abate JP, Dilks K, Landis J, Ashraf J, Murphy CT, et al. Condition-adapted stress
517 and longevity gene regulation by Caenorhabditis elegans SKN-1/Nrf. Aging Cell. 2009;8(5):524-41.
518 Epub 2009/07/07. doi: ACE501 [pii]
519 10.1111/j.1474-9726.2009.00501.x. PubMed PMID: 19575768.
520 33. Park SK, Tedesco PM, Johnson TE. Oxidative stress and longevity in Caenorhabditis elegans as
521 mediated by SKN-1. Aging Cell. 2009;8(3):258-69. Epub 2009/07/25. doi: 10.1111/j.1474-
522 9726.2009.00473.x. PubMed PMID: 19627265; PubMed Central PMCID: PMC2762118.
523 34. An JH, Blackwell TK. SKN-1 links C. elegans mesendodermal specification to a conserved
524 oxidative stress response. Genes Dev. 2003;17(15):1882-93. Epub 2003/07/19. doi:
525 10.1101/gad.1107803. PubMed PMID: 12869585.
526 35. Horsman JW, Heinis FI, Miller DL. A Novel Mechanism To Prevent H2S Toxicity in
527 Caenorhabditis elegans. Genetics. 2019;213(2):481-90. doi: 10.1534/genetics.119.302326. PubMed
528 PMID: 31371406; PubMed Central PMCID: PMCPMC6781907.
529 36. Li WH, Chang CH, Huang CW, Wei CC, Liao VH. Selenite enhances immune response against

530 Pseudomonas aeruginosa PA14 via SKN-1 in Caenorhabditis elegans. PLoS One. 2014;9(8):e105810.
531 doi: 10.1371/journal.pone.0105810. PubMed PMID: 25147937; PubMed Central PMCID:
532 PMCPMC4141825.
533 37. Miller DL, Budde MW, Roth MB. HIF-1 and SKN-1 coordinate the transcriptional response to
534 hydrogen sulfide in Caenorhabditis elegans. PLoS One. 2011;6(9):e25476. Epub 2011/10/08. doi:
535 10.1371/journal.pone.0025476
536 PONE-D-11-09953 [pii]. PubMed PMID: 21980473; PubMed Central PMCID: PMC3183046.
537 38. Kamath RS, Ahringer J. Genome-wide RNAi screening in Caenorhabditis elegans. Methods.
538 2003;30(4):313-21. Epub 2003/06/28. doi: S1046202303000501 [pii]. PubMed PMID: 12828945.
539 39. Inoue H, Hisamoto N, An JH, Oliveira RP, Nishida E, Blackwell TK, et al. The C. elegans p38
540 MAPK pathway regulates nuclear localization of the transcription factor SKN-1 in oxidative stress
541 response. Genes Dev. 2005;19(19):2278-83. Epub 2005/09/17. doi: gad.1324805 [pii]
542 10.1101/gad.1324805. PubMed PMID: 16166371.
543 40. Zhang Y, Shao Z, Zhai Z, Shen C, Powell-Coffman JA. The HIF-1 hypoxia-inducible factor
544 modulates lifespan in C. elegans. PLoS One. 2009;4(7):e6348. Epub 2009/07/28. doi:
545 10.1371/journal.pone.0006348. PubMed PMID: 19633713.
546 41. Padilla PA, Nystul TG, Zager RA, Johnson AC, Roth MB. Dephosphorylation of cell cycle-
547 regulated proteins correlates with anoxia-induced suspended animation in Caenorhabditis elegans. Mol
548 Biol Cell. 2002;13(5):1473-83. Epub 2002/05/15. doi: 10.1091/mbc.01-12-0594. PubMed PMID:
549 12006646.
550 42. Li X, Matilainen O, Jin C, Glover-Cutter KM, Holmberg CI, Blackwell TK. Specific SKN-1/Nrf
551 stress responses to perturbations in translation elongation and proteasome activity. PLoS Genet.
552 2011;7(6):e1002119. Epub 2011/06/23. doi: 10.1371/journal.pgen.1002119. PubMed PMID: 21695230;
553 PubMed Central PMCID: PMC3111486.
554 43. Tullet JM, Hertweck M, An JH, Baker J, Hwang JY, Liu S, et al. Direct inhibition of the
555 longevity-promoting factor SKN-1 by insulin-like signaling in C. elegans. Cell. 2008;132(6):1025-38.
556 Epub 2008/03/25. doi: S0092-8674(08)00130-X [pii]
557 10.1016/j.cell.2008.01.030. PubMed PMID: 18358814.
558 44. Wang J, Robida-Stubbs S, Tullet JM, Rual JF, Vidal M, Blackwell TK. RNAi screening
559 implicates a SKN-1-dependent transcriptional response in stress resistance and longevity deriving from
560 translation inhibition. PLoS Genet. 2010;6(8). Epub 2010/08/12. doi: 10.1371/journal.pgen.1001048.
561 PubMed PMID: 20700440; PubMed Central PMCID: PMC2916858.
562 45. Darby C, Cosma CL, Thomas JH, Manoil C. Lethal paralysis of Caenorhabditis elegans by
563 Pseudomonas aeruginosa. Proc Natl Acad Sci U S A. 1999;96(26):15202-7. Epub 1999/12/28. PubMed
564 PMID: 10611362.
565 46. Niu W, Lu ZJ, Zhong M, Sarov M, Murray JI, Brdlik CM, et al. Diverse transcription factor
566 binding features revealed by genome-wide ChIP-seq in C. elegans. Genome research. 2011;21(2):245-54.
567 Epub 2010/12/24. doi: 10.1101/gr.114587.110. PubMed PMID: 21177963; PubMed Central PMCID:
568 PMC3032928.
569 47. Glover-Cutter KM, Lin S, Blackwell TK. Integration of the unfolded protein and oxidative stress
570 responses through SKN-1/Nrf. PLoS Genet. 2013;9(9):e1003701. doi: 10.1371/journal.pgen.1003701.
571 PubMed PMID: 24068940; PubMed Central PMCID: PMCPMC3772064.
572 48. Paek J, Lo JY, Narasimhan SD, Nguyen TN, Glover-Cutter K, Robida-Stubbs S, et al.
573 Mitochondrial SKN-1/Nrf mediates a conserved starvation response. Cell Metab. 2012;16(4):526-37. doi:
574 10.1016/j.cmet.2012.09.007. PubMed PMID: 23040073; PubMed Central PMCID: PMCPMC3774140.
575 49. Robida-Stubbs S, Glover-Cutter K, Lamming DW, Mizunuma M, Narasimhan SD, Neumann-
576 Haefelin E, et al. TOR signaling and rapamycin influence longevity by regulating SKN-1/Nrf and DAF-
577 16/FoxO. Cell Metab. 2012;15(5):713-24. doi: 10.1016/j.cmet.2012.04.007. PubMed PMID: 22560223;
578 PubMed Central PMCID: PMCPMC3348514.
579 50. Bishop NA, Guarente L. Two neurons mediate diet-restriction-induced longevity in C. elegans.
580 Nature. 2007;447(7144):545-9. Epub 2007/06/01. doi: nature05904 [pii]

581 10.1038/nature05904. PubMed PMID: 17538612.
582 51. Chen D, Thomas EL, Kapahi P. HIF-1 modulates dietary restriction-mediated lifespan extension
583 via IRE-1 in Caenorhabditis elegans. PLoS Genet. 2009;5(5):e1000486. Epub 2009/05/23. doi:
584 10.1371/journal.pgen.1000486. PubMed PMID: 19461873.
585 52. Park EC, Ghose P, Shao Z, Ye Q, Kang L, Xu XZ, et al. Hypoxia regulates glutamate receptor
586 trafficking through an HIF-independent mechanism. The EMBO journal. 2012;31(6):1379-93. Epub
587 2012/01/19. doi: 10.1038/emboj.2011.499. PubMed PMID: 22252129; PubMed Central PMCID:
588 PMC3321172.
589 53. Pocock R, Hobert O. Oxygen levels affect axon guidance and neuronal migration in
590 Caenorhabditis elegans. Nat Neurosci. 2008;11(8):894-900. Epub 2008/07/01. doi: nn.2152 [pii]
591 10.1038/nn.2152. PubMed PMID: 18587389.
592 54. Chang AJ, Bargmann CI. Hypoxia and the HIF-1 transcriptional pathway reorganize a neuronal
593 circuit for oxygen-dependent behavior in Caenorhabditis elegans. Proc Natl Acad Sci U S A.
594 2008;105(20):7321-6. doi: 10.1073/pnas.0802164105. PubMed PMID: 18477695; PubMed Central
595 PMCID: PMCPMC2438248.
596 55. Lin HC, Su SL, Lu CY, Lin AH, Lin WC, Liu CS, et al. Andrographolide inhibits hypoxia-
597 induced HIF-1alpha-driven endothelin 1 secretion by activating Nrf2/HO-1 and promoting the expression
598 of prolyl hydroxylases 2/3 in human endothelial cells. Environ Toxicol. 2017;32(3):918-30. doi:
599 10.1002/tox.22293. PubMed PMID: 27297870.
600 56. Duarte TL, Talbot NP, Drakesmith H. NRF2 and Hypoxia-Inducible Factors: Key Players in the
601 Redox Control of Systemic Iron Homeostasis. Antioxid Redox Signal. 2020. doi: 10.1089/ars.2020.8148.
602 PubMed PMID: 32791852.
603 57. Li L, Pan H, Wang H, Li X, Bu X, Wang Q, et al. Interplay between VEGF and Nrf2 regulates
604 angiogenesis due to intracranial venous hypertension. Sci Rep. 2016;6:37338. doi: 10.1038/srep37338.
605 PubMed PMID: 27869147; PubMed Central PMCID: PMCPMC5116754.
606 58. Wong BW, Kuchnio A, Bruning U, Carmeliet P. Emerging novel functions of the oxygen-sensing
607 prolyl hydroxylase domain enzymes. Trends Biochem Sci. 2013;38(1):3-11. doi:
608 10.1016/j.tibs.2012.10.004. PubMed PMID: 23200187.
609 59. Bellier A, Chen CS, Kao CY, Cinar HN, Aroian RV. Hypoxia and the hypoxic response pathway
610 protect against pore-forming toxins in C. elegans. PLoS Pathog. 2009;5(12):e1000689. Epub 2009/12/17.
611 doi: 10.1371/journal.ppat.1000689. PubMed PMID: 20011506.
612 60. Lee SS, Lee RY, Fraser AG, Kamath RS, Ahringer J, Ruvkun G. A systematic RNAi screen
613 identifies a critical role for mitochondria in C. elegans longevity. Nat Genet. 2003;33(1):40-8. Epub
614 2002/11/26. doi: 10.1038/ng1056
615 ng1056 [pii]. PubMed PMID: 12447374.
616 61. Hansen M, Hsu AL, Dillin A, Kenyon C. New genes tied to endocrine, metabolic, and dietary
617 regulation of lifespan from a Caenorhabditis elegans genomic RNAi screen. PLoS Genet. 2005;1(1):119-
618 28. Epub 2005/08/17. doi: 10.1371/journal.pgen.0010017. PubMed PMID: 16103914; PubMed Central
619 PMCID: PMC1183531.
620 62. Hamilton B, Dong Y, Shindo M, Liu W, Odell I, Ruvkun G, et al. A systematic RNAi screen for
621 longevity genes in C. elegans. Genes Dev. 2005;19(13):1544-55. Epub 2005/07/07. doi: 19/13/1544 [pii]
622 10.1101/gad.1308205. PubMed PMID: 15998808.
623 63. Curran SP, Ruvkun G. Lifespan regulation by evolutionarily conserved genes essential for
624 viability. PLoS Genet. 2007;3(4):e56. Epub 2007/04/07. doi: 07-PLGE-RA-0112R1 [pii]
625 10.1371/journal.pgen.0030056. PubMed PMID: 17411345.
626 64. Kim Y, Sun H. Functional genomic approach to identify novel genes involved in the regulation of
627 oxidative stress resistance and animal lifespan. Aging Cell. 2007;6(4):489-503. Epub 2007/07/05. doi:
628 ACE302 [pii]
629 10.1111/j.1474-9726.2007.00302.x. PubMed PMID: 17608836.
630 65. Sugimoto T, Mori C, Takanami T, Sasagawa Y, Saito R, Ichiishi E, et al. Caenorhabditis elegans
631 par2.1/mtssb-1 is essential for mitochondrial DNA replication and its defect causes comprehensive

632 transcriptional alterations including a hypoxia response. Experimental cell research. 2008;314(1):103-14.
633 Epub 2007/09/29. doi: 10.1016/j.yexcr.2007.08.015. PubMed PMID: 17900564.
634 66. Lamitina T, Huang CG, Strange K. Genome-wide RNAi screening identifies protein damage as a
635 regulator of osmoprotective gene expression. Proc Natl Acad Sci U S A. 2006;103(32):12173-8. Epub
636 2006/08/02. doi: 0602987103 [pii]
637 10.1073/pnas.0602987103. PubMed PMID: 16880390.
638 67. Nollen EA, Garcia SM, van Haaften G, Kim S, Chavez A, Morimoto RI, et al. Genome-wide
639 RNA interference screen identifies previously undescribed regulators of polyglutamine aggregation. Proc
640 Natl Acad Sci U S A. 2004;101(17):6403-8. Epub 2004/04/16. doi: 10.1073/pnas.0307697101
641 0307697101 [pii]. PubMed PMID: 15084750.
642 68. Selak MA, Armour SM, MacKenzie ED, Boulahbel H, Watson DG, Mansfield KD, et al.
643 Succinate links TCA cycle dysfunction to oncogenesis by inhibiting HIF-alpha prolyl hydroxylase.
644 Cancer Cell. 2005;7(1):77-85. Epub 2005/01/18. doi: S153561080400368X [pii]
645 10.1016/j.ccr.2004.11.022. PubMed PMID: 15652751.
646 69. Koivunen P, Hirsila M, Remes AM, Hassinen IE, Kivirikko KI, Myllyharju J. Inhibition of
647 hypoxia-inducible factor (HIF) hydroxylases by citric acid cycle intermediates: possible links between
648 cell metabolism and stabilization of HIF. The Journal of biological chemistry. 2007;282(7):4524-32.
649 Epub 2006/12/22. doi: M610415200 [pii]
650 10.1074/jbc.M610415200. PubMed PMID: 17182618.
651 70. Walker AK, Jacobs RL, Watts JL, Rottiers V, Jiang K, Finnegan DM, et al. A conserved SREBP-
652 1/phosphatidylcholine feedback circuit regulates lipogenesis in metazoans. Cell. 2011;147(4):840-52.
653 Epub 2011/11/01. doi: 10.1016/j.cell.2011.09.045. PubMed PMID: 22035958; PubMed Central PMCID:
654 PMC3384509.
655 71. Simmer F, Moorman C, van der Linden AM, Kuijk E, van den Berghe PV, Kamath RS, et al.
656 Genome-wide RNAi of C. elegans using the hypersensitive rrf-3 strain reveals novel gene functions.
657 PLoS Biol. 2003;1(1):E12. Epub 2003/10/14. doi: 10.1371/journal.pbio.0000012. PubMed PMID:
658 14551910; PubMed Central PMCID: PMC212692.
659 72. Blackwell TK, Bowerman B, Priess JR, Weintraub H. Formation of a monomeric DNA binding
660 domain by Skn-1 bZIP and homeodomain elements. Science. 1994;266(5185):621-8. Epub 1994/10/28.
661 PubMed PMID: 7939715.
662 73. Mello CC, Kramer JM, Stinchcomb D, Ambros V. Efficient gene transfer in C.elegans:
663 extrachromosomal maintenance and integration of transforming sequences. The EMBO journal.
664 1991;10(12):3959-70. Epub 1991/12/01. PubMed PMID: 1935914.
665 74. Pfaffl MW. A new mathematical model for relative quantification in real-time RT-PCR. Nucleic
666 Acids Res. 2001;29(9):e45. Epub 2001/05/09. PubMed PMID: 11328886; PubMed Central PMCID:
667 PMC55695.
668

669 # Supporting information

670 **S1 Fig. *nhr-57* promoter HIF-1 chromatin immunoprecipitation experiments.** (A) *nhr-57*

671 promoter sequence and positions of primers used for real-time quantitative PCR assays in HIF-1

672 chromatin immunoprecipitation experiments. (B) Primer sequences for real-time quantitative PCR assays

673 in *nhr-57* promoter HIF-1 chromatin immunoprecipitation experiments. (C) Chromatin co-

674 immunoprecipitation data. In these experiments the endogenous *hif-1* locus was disrupted by the
675 *ia04* large deletion and HIF-1 function was restored by the *Phif-1:hif-1a:Myc:HA* transgene [40].
676 The relative amounts of *nhr-57* promoter regions that co-immunoprecipitated with HIF-
677 1:Myc:HA was determined by real-time quantitative PCR. The bars show the average enriched
678 fold from at least three independent replicates. *inf-1*, a gene not regulated by HIF-1, was used as
679 the reference gene.

680 **S2 Fig. RNAi inactivation of *sams-1* or *sbp-1* increased *Pnhr-57:GFP* expression.** (A) RNAi
681 for *sams-1* (S-adenosyl methionine synthetase) increased *Pnhr-57*:*GFP* expression more than 7-
682 fold in animals carrying the wild-type *hif-1* allele relative to control RNAi, and increased the
683 reporter 3-fold in animals carrying the *hif-1(ia04)* deletion. The difference in RNAi effect
684 between *hif-1(+)* and *hif-1(ia04)* strains is statistically significant (*$p < 0.05$, from six
685 independent experiments, by student *t*-test). (B) RNAi for the SREBP homolog *sbp-1* increased
686 expression of the reporter more than 3-fold in animals carrying the wild-type *hif-1* allele, but had
687 no effect on *Pnhr-57*:*GFP* expression in *hif-1(ia04)* mutants. The difference in RNAi effect
688 between *hif-1(+)* and *hif-1(ia04)* strains is statistically significant (*$p < 0.05$, from five
689 independent experiments, by student *t*-test). GFP levels were determined by protein blots, and
690 the control animals were fed on bacteria carrying the empty RNAi vector (L4440). The
691 experiments were conducted in RNAi-sensitive strains (*rrf-3(pk1426*)).

692 **S1 Table. Genes increased *Pnhr-57:GFP* expression when knocked-down by RNAi.**

693 **S2 Table. Genes for which RNAi caused *hif-1*-dependent increase of *Pnhr-57:GFP***
694 **expression.**

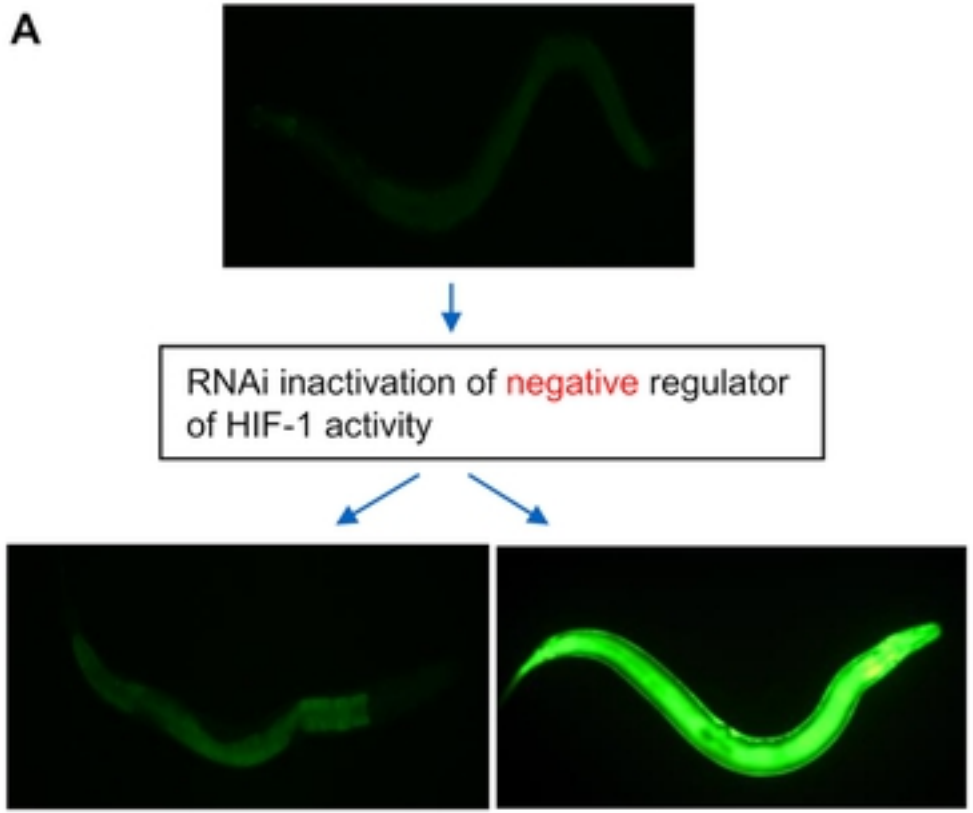
A
RNAi inactivation of negative regulator of HIF-1 activity

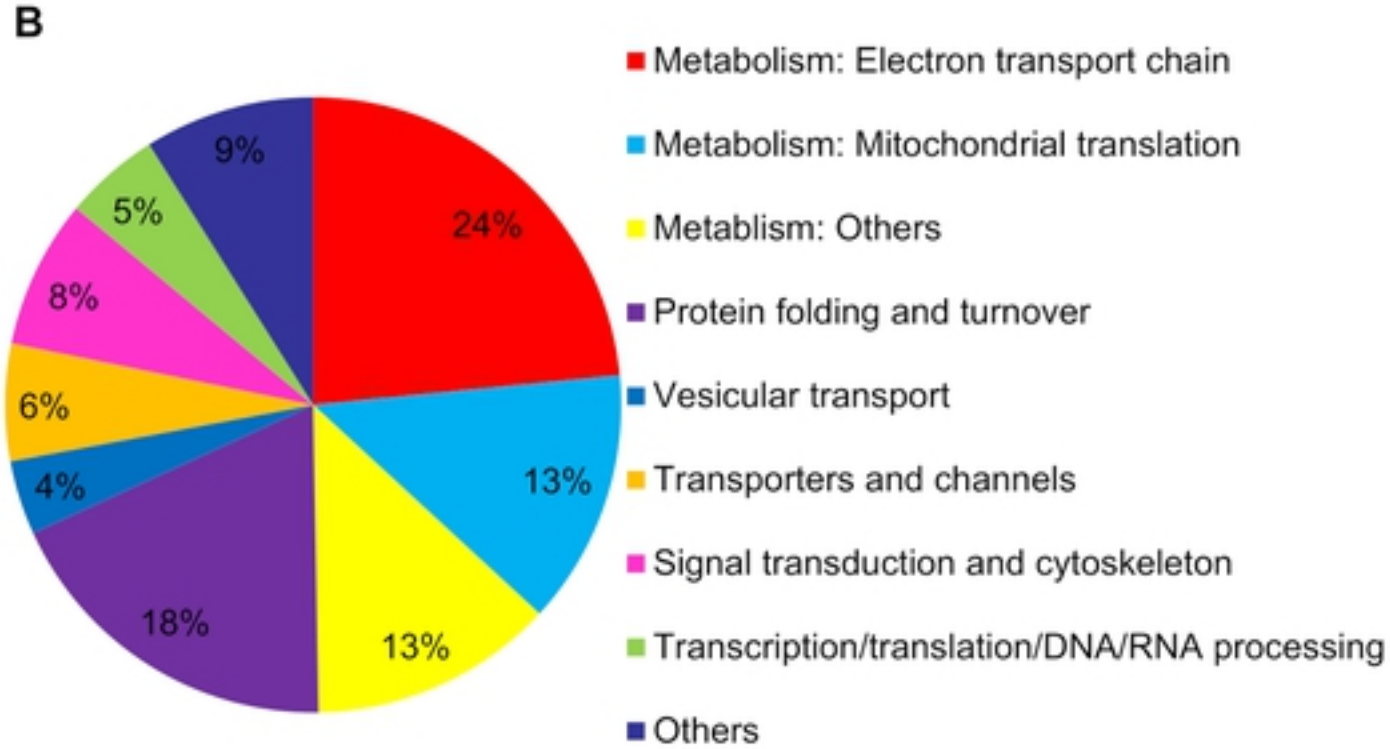
B
24%
13%
13%
18%
4%
6%
8%
5%
9%
Metabolism: Electron transport chain
Metabolism: Mitochondrial translation
Metablism: Others
Protein folding and turnover
Vesicular transport
Transporters and channels
Signal transduction and cytoskeleton
Transcription/translation/DNA/RNA processing
Others

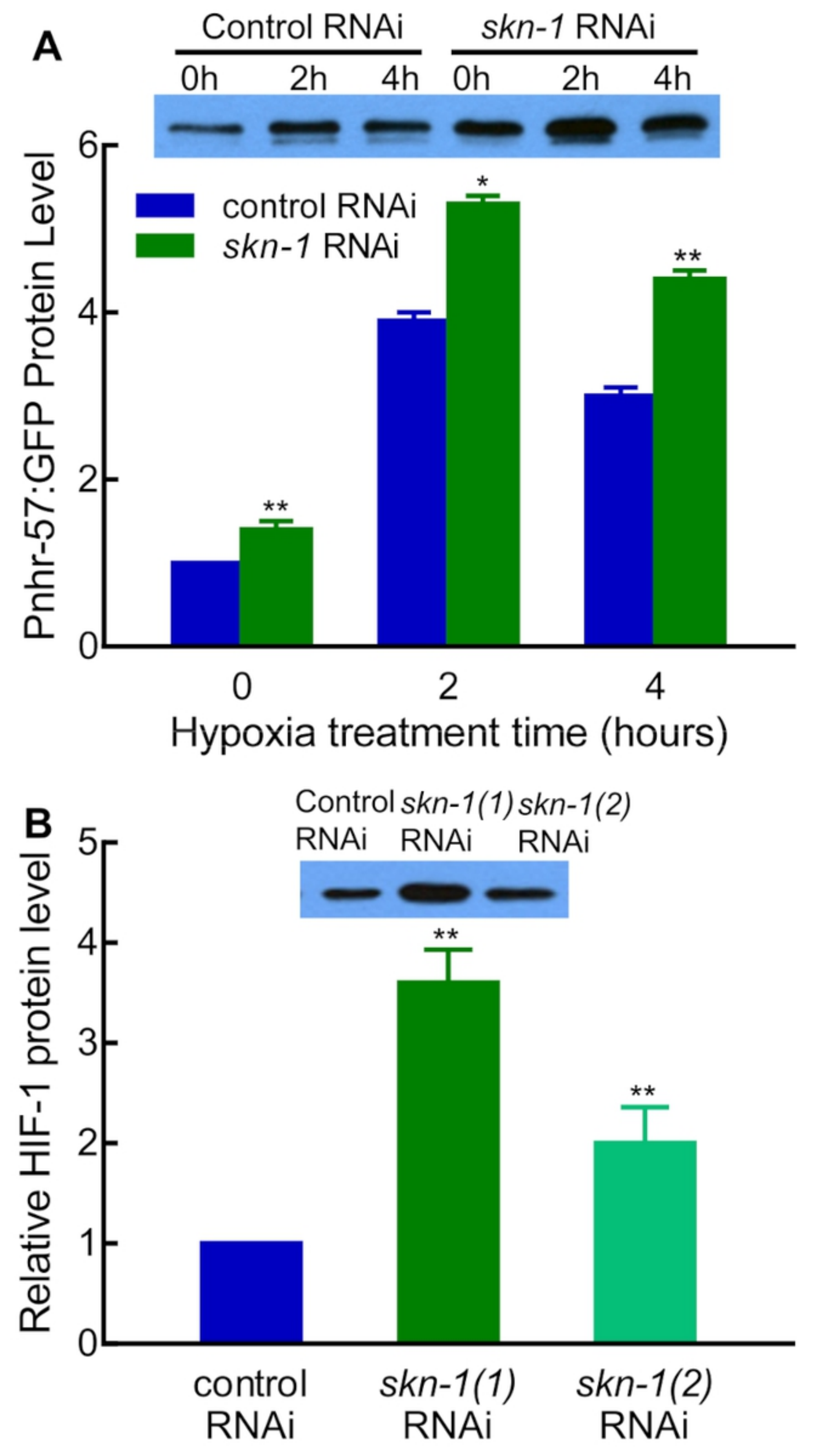
A
Control RNAi
skn-1 RNAi
0h
2h
4h
0h
2h
4h
Pnhr-57:GFP Protein Level
control RNAi
skn-1 RNAi
*
**
**
0
2
4
6
0
2
4
Hypoxia treatment time (hours)
B
Control RNAi
skn-1(1) RNAi
skn-1(2) RNAi
Relative HIF-1 protein level
**
**
0
1
2
3
4
5
control RNAi
skn-1(1) RNAi
skn-1(2) RNAi

A

```
egl-9 -365 CTTTGTCATCGTGTCTCTTTGATCCG -340
gcs-1 -122 CTTTATCATCATGA-GATTTAATGTT -98
med-1 -124 CTCTGTCATCATGATGATTTTTGGAG -99
med-2 -124 CTCTGTCATCATGATGATTTTTAGAG -99
           ** * ***** **     ***
```

B

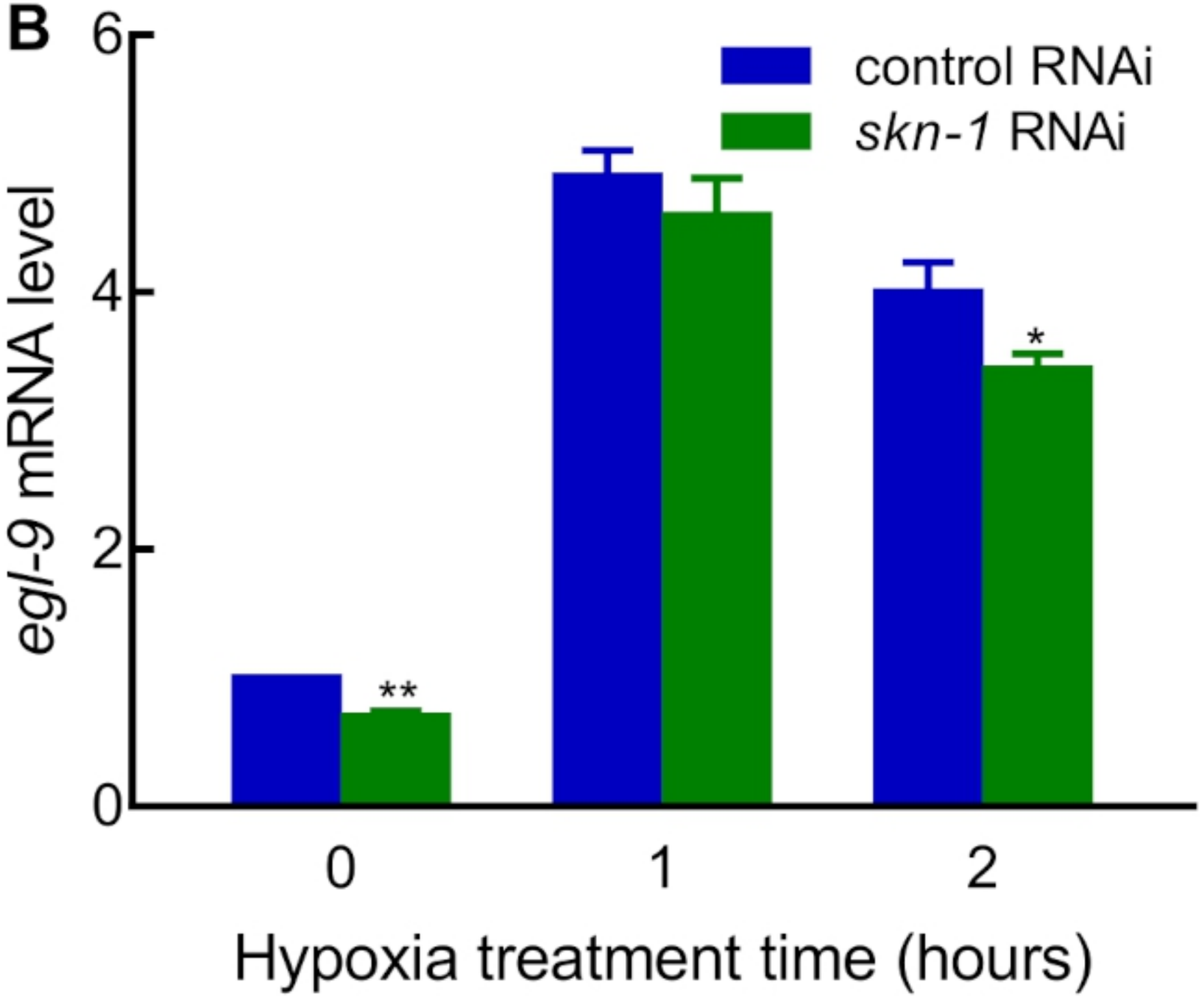

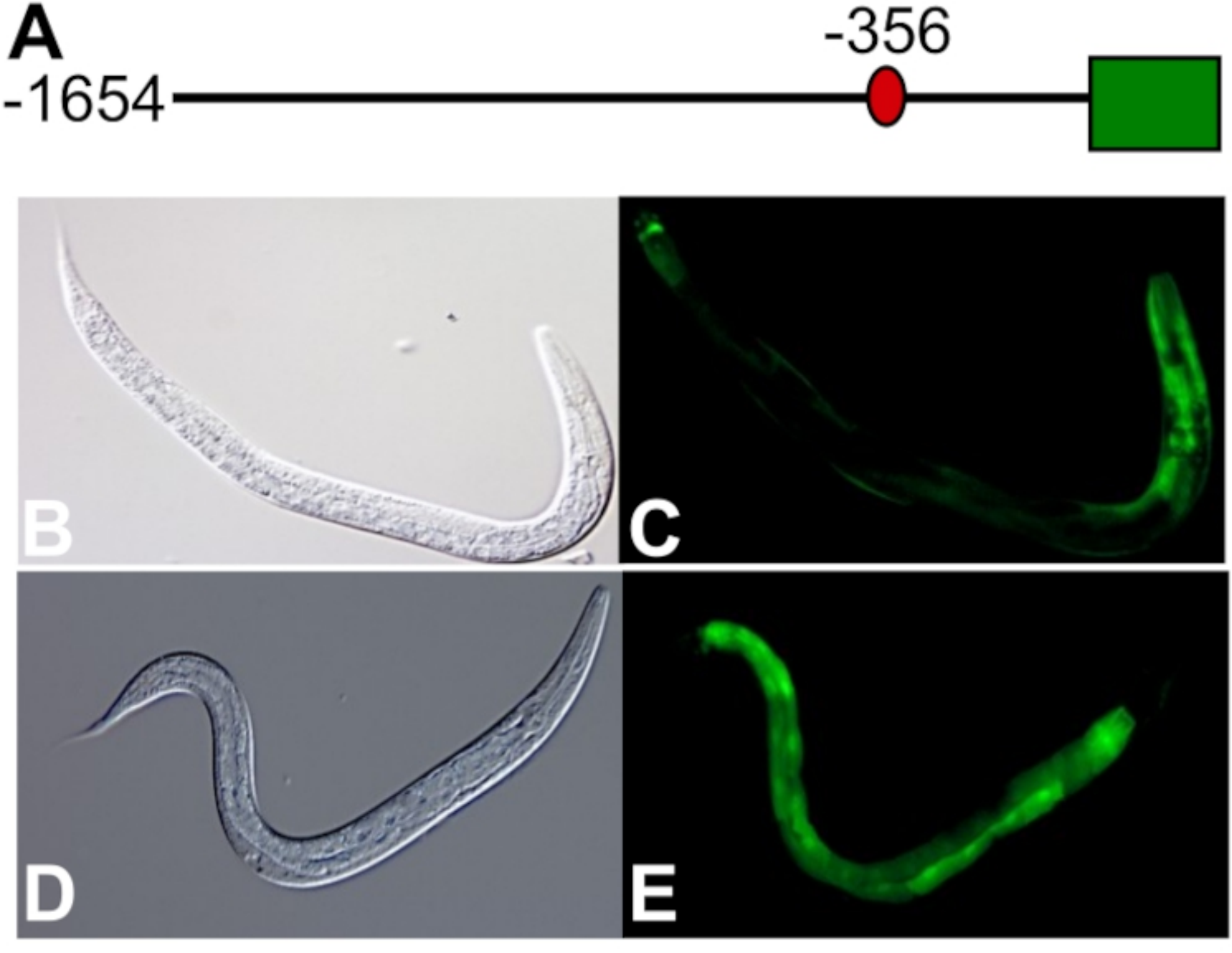
A
-356
-1654
B
C
D
E

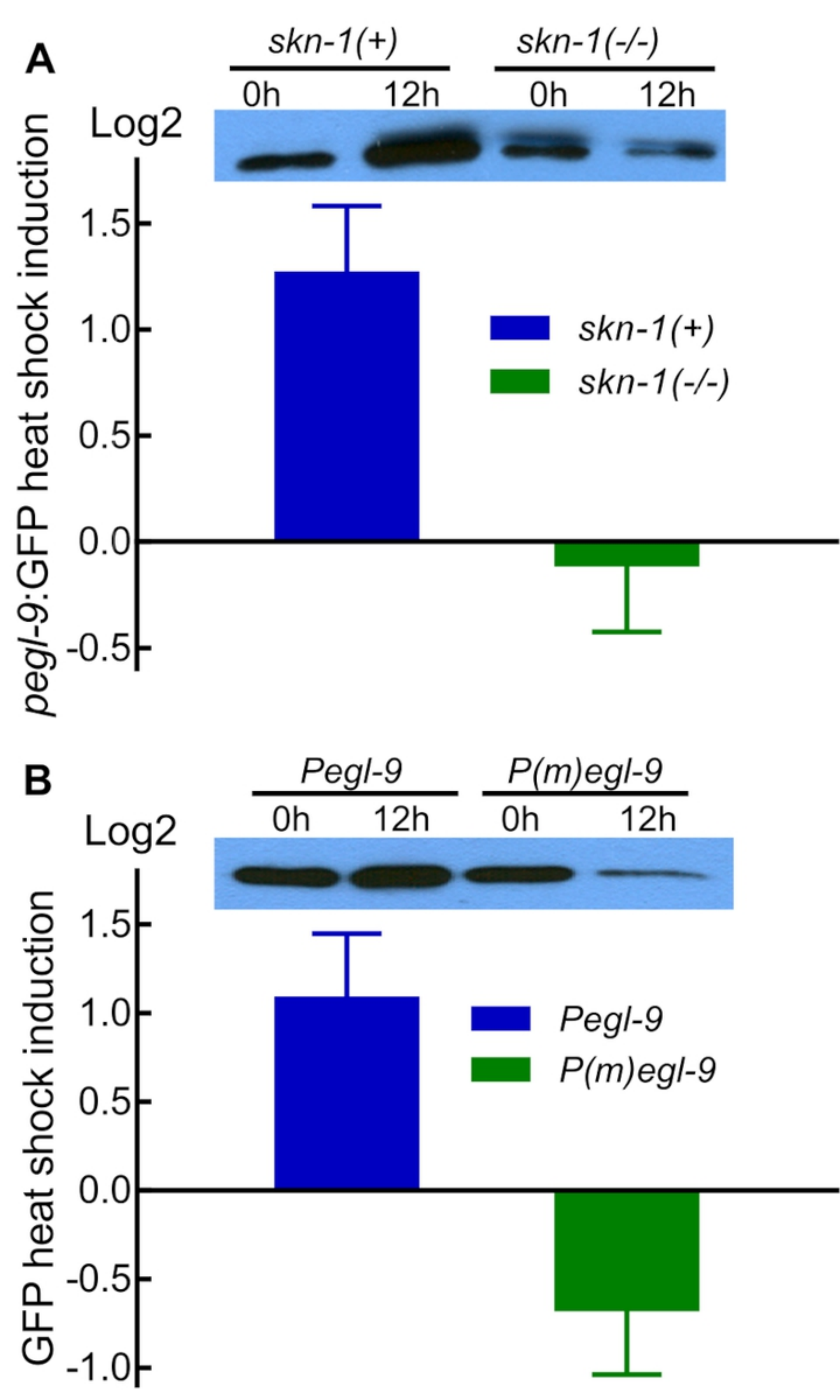
A
skn-1(+)
skn-1(-/-)
0h
12h
0h
12h
Log2
pegl-9:GFP heat shock induction
1.5
1.0
0.5
0.0
-0.5
skn-1(+)
skn-1(-/-)
B
Pegl-9
P(m)egl-9
0h
12h
0h
12h
Log2
GFP heat shock induction
1.5
1.0
0.5
0.0
-0.5
-1.0
Pegl-9
P(m)egl-9